euspen's 22nd International Conference & Exhibition, Geneva, CH, May/June 2022
www.euspen.eu

Simulation-based investigation of the interaction between tool and workpiece in grinding with micro pencil grinding tools

Andreas Lange[1], Daniel Müller[1], Benjamin Kirsch[1], Jan C. Aurich[1]

[1]*Technische Universität Kaiserslautern; Institute for Manufacturing Technology and Production Systems*

andreas.lange@mv.uni-kl.de

Abstract
In micro manufacturing, the influence of the tool spindle on the process and tool dynamics is predominant. Furthermore, the cutting tools used possess low stiffnesses due to their size. In order to improve part quality, it is necessary to know whether the tool path is influenced by process-machine-interactions, process-tool-interactions or a single factor. In this contribution, a coupled simulation model is set up to analyse the influences of cutting forces, tool dynamics, and spindle dynamics on the tool motion in grinding with micro pencil grinding tools. For this purpose, an axisymmetric dynamic spindle model is coupled with a three-dimensional dynamic tool model. Cutting forces are measured and implemented as a boundary condition within the coupled simulation model. Using this model, the tool motion is compared for three different cases: without the implementation of cutting forces, with the implementation of cutting forces but without variation of the cutting forces due to interactions, and with the implementation of cutting forces and interactions. The results show that in grinding with micro pencil grinding tools, the tool motion is influenced by the cutting forces and the spindle dynamics. However, the spindle dynamics are not significantly influenced by the tool deformation and cutting forces. It can be concluded that in grinding with micro pencil grinding tools, only process-tool-interactions and an influence of the spindle dynamics can be observed, but no process-machine-interactions.

Micromachining, Finite element method (FEM), Spindle, Vibration

1. Introduction

Process-machine interactions (PMI) can affect both the machine tool, especially the tool spindle, and the process result [1]. Therefore, the investigation and suppression of PMI has already been extensively studied in macro machining [2]. However, micro machining differs, among other things, in the changed dimensional ratios between tool spindle, tool and chip. For this reason, methods for studying PMI in macro machining cannot be readily applied to micro machining [3]. Instead, the tool spindle and the tool must be considered as separate aspects [4] to allow differentiation between spindle influence, tool influence, PMI, and process-tool interaction (PTI).

With the help of a simulation-based investigation of the tool spindle, the tool and the process forces, it is possible to investigate the influence of individual parameters and their effects on PMI/PTI. However, in contrast to simulation-based investigations of micro milling [5, 6], it is difficult to integrate a suitable model to consider grinding forces due to the geometrically undefined cutting edges of the grinding tool. The implementation of measured grinding forces allows the cutting forces to be taken into account and thus the individual influences and interactions to be determined and differentiated.

Further, due to the geometrically undefined cutting edges, the grit geometry must be either measured [7] and converted to a suitable model, or a specific grit shape must be assumed. Several works focus on the investigation of the grit shapes. For example, in [8], a finite-element-model is used to model grinding forces in micro grinding. Herein spherical, ellipsoidal, pyramid-shaped, and frustum-pyramid-shaped grits are compared to analyse the influence of the grits' shape on the generated forces. In [9], four different grit shapes (sphere, truncated cone, cone) are compared to analyse the generated workpiece surface.

This paper describes a method to investigate the process-tool interaction during grinding with micro pencil grinding tools. For this purpose, grinding forces are measured and integrated into a simulation model of a tool spindle and a tool. With the help of the simulation model, the influence of the tool spindle and the cutting forces on the tool motion is investigated. Furthermore, a distinction is made as to whether this is the result of individual parameter influences, PTI or PMI.

2. Methods

2.1. Measurement of cutting forces

Electroless plated micro pencil grinding tools were used for the experiments. The tools consisted of a steel base body with a diameter of 20 µm. The base body was used as a substrate for the abrasive layer. This abrasive layer consisted of a nickel-phosphorous alloy matrix containing cubic boron nitride (cBN) grits with a nominal size of 5-10 µm. The layer thickness was approximately 15 µm, giving an effective tool diameter of 50 µm. A cavity was incorporated in the center of the front face of the tool. This was to prevent contact between the workpiece and the tool near the rotational axis and hence to prevent ploughing and the formation of substructures at the slot bottom [10]. The abrasive layer had a density of 8.5 g/cm^3 [11], a Young's modulus of 180 GPa [12], and a Possion's ratio of 0.315 [12]. A schematic view of the tool is given in figure 1a). The experimental investigations were carried out on a four-axes desktop-sized machine tool. An air bearing spindle (schematic view is given in figure 1b)) with a spindle rotational speed range between 15,000 min^{-1} and 160,000 min^{-1} was used. The cutting forces were measured using

a dynamometer (Kistler[1], MiniDyn Type 9119AA1; sensitivity < 2 mN, natural frequency < 6 kHz). 16MnCr5 (660 HV 30) was used as the workpiece material and an immersion cooling lubrication was used [13].

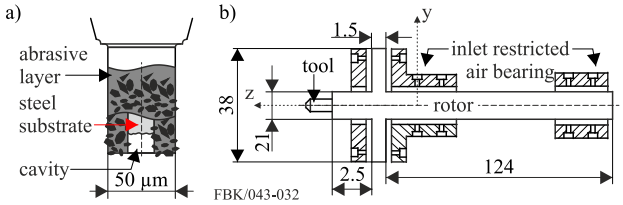

Figure 1. Schematic view of the tool and the machine tool spindle

Pendulum grinding was carried out using three different rotational speeds: 30,000 min^{-1}, 90,000 min^{-1}, and 150,000 min^{-1}. The cutting depth for all cuts was kept constant at 0.5 µm. Ten cuts per slot were machined, giving a final target slot depth of 5 µm. All measurements were repeated three times. Before each measurement, the rotational speed was kept constant until a possible (further) thermal growth could be ruled out. Figure 2 shows the measured cutting forces in x-,y-, and z-direction. As can be seen, the axial forces (z-direction) are larger than the lateral forces by approximately one magnitude. Additionally, the standard deviation is rather high.

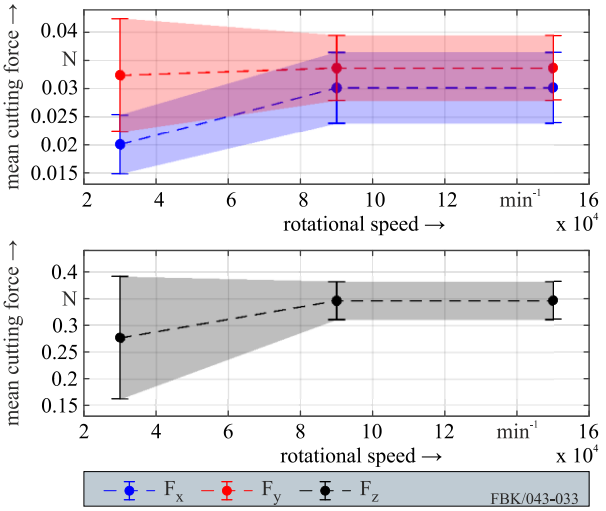

Figure 2. Measured cutting forces (mean values)

2.2. Simulation setup

The simulation setup consists of an axisymmetric finite element model of the machine tool spindle, a supplementary finite element model of the inlet restricted air bearings and a three-dimensional dynamic tool model. An additional boundary condition is implemented for the application of the cutting forces. A schematic view of the micro pencil grinding tool and the modelled machine tool spindle is given in figure 1.

The finite element model of the air bearings is based on the work in [14] and is used to compute the corresponding dynamic stiffness and damping coefficients of the bearings. The finite element model of the tool spindle, more precisely of the rotor excluding the tool, is based on the work in [15] and is used as foundation for this work. Axisymmetric finite elements are used for the modelling of the rotor. The drive motor, as in electromagnetic effects, is not modelled. The mass unbalance force $\{f_u\}$ is defined in the x-y-plane by the following equation:

$$\{f_u\} = m\varepsilon \begin{Bmatrix} \dot{\Omega}\sin(\Omega t) + \Omega^2\cos(\Omega t) \\ -\dot{\Omega}\cos(\Omega t) + \Omega^2\sin(\Omega t) \end{Bmatrix} \qquad (1)$$

where m is the rotating unbalanced mass, ε is the eccentricity, Ω is the angular velocity, and $\dot{\Omega}$ is the rotational acceleration. The value of the unbalance force was determined and validated in [15]. A comparison between the measured cutting forces in x- and y-direction and the unbalance force is shown in table 1. As can be seen, the cutting forces are small compared to the unbalance force at all rotational speeds, implying that the cutting forces may only play a minor role regarding the rotor`s motion.

The dynamic tool model is set up using standard three-dimensional finite elements in order to model the grits and for the application of unevenly distributed cutting forces. The measured cutting forces are applied at the end face of the micro pencil grinding tool. Since the grinding forces are implemented as a measured boundary condition, they also include force components resulting from ploughing. Overall, it can be assumed that multiple grits are in contact with the workpiece. Here, five grits were modelled and distributed equidistantly over the circumference of the tool. As the subject of interest in this study is the interaction between tool and workpiece and not the exact surface generation, a simple cube shape can be assumed for the grits without the need to investigate different grit shapes, unlike in [8] and [9].

Table 1. Comparison between averaged measured cutting forces and unbalance forces

rotational speed/min^{-1}	cutting forces (magnitude)/N	unbalance force/N	ratio
30,000	0.036	0.41	0.088
90,000	0.042	3.69	0.011
150,000	0.042	10.24	0.004

2.3. Implementation of cutting forces

The measured cutting forces already include PMI/PTI effects as they cannot be omitted during experiments. However, the percentage by which the PMI/PTI effects affect these measured cutting force values is unknown. As such, it is necessary to model the ideal cutting forces (no change of forces due to PMI/PTI effects and tool deformation) to differentiate between PTI due to the sole consideration of cutting forces and PMI/PTI due to cutting forces and additional PMI/PTI (caused by ongoing cutting force variations due to tool deformations and vice versa).

To model the ideal cutting forces, the measured cutting forces are curve fitted. Assuming that the ideal cutting forces have a periodic pattern, they can be modelled using a sum of sines model, which is given by:

$$f(x) = \sum_{i=1}^{n} a_i \cdot \sin(b_i x + c_i) \qquad (2)$$

where a is the amplitude, b is the frequency, c is the phase constant for each sine wave term, and n is the number of terms in the series. For this analysis, the parameters are fitted using the MATLAB[1] curve fitting toolbox[1]. For the measured cutting forces shown in figure 3, the computed curve fitting values are: $a_1 = 0.10$, $b_1 = 19.6$, $c_1 = -2.76$, and n is chosen as 1.

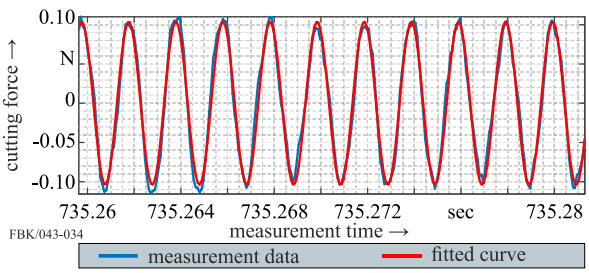

Figure 3. Measured cutting forces and fitted cutting force curve in y-direction at a rotational speed of 30,000 min^{-1}

Additional simulations are set up, where the measured cutting forces are scaled up to investigate the effects of higher cutting forces, for example due to higher depths of cut. Here, the scaling factors were chosen between 2 and 5 (integer numbers only).

3. Results

In the following sections, the term motion represents the totality of deformation (bending, compression, etc.) and rigid-body motion due to all applied forces (including unbalance forces). The term tool deformation refers to the deformation of the tool due to applied cutting forces.

Figure 4 shows a comparison between the motion in y-direction with and without the consideration of cutting forces and PMI/PTI effects at four different mesh nodes. Three different rotational speeds are evaluated. For each rotational speed, six bars are shown. From left to right, these bars show the maximum motion amplitude without cutting forces (only rotordynamic effects considered), with the measured cutting forces, and with the scaled measured cutting forces to simulate the effects of higher depths of cuts. The motion in x-direction is similar, both in terms of overall behaviour and amplitude, and thus not shown here.

The highest motion amplitudes are found at 90,000 min^{-1} due to an eigenfrequency of the rotor near this speed (at approximately 78,000 min^{-1}). The influence of the spindle dynamics on the process dynamics without the consideration of clamping and tool shaft roundness errors can be determined from the maximum motion amplitudes at node 1 at no cutting forces (mind the different scales). The corresponding amplitudes are 0.05 µm, 1.47 µm, and 0.57 µm for the three depicted rotational speeds. Thus, it can be stated that the rotordynamic behaviour of the spindle shaft influences the tool motion. Whether this influence is significant depends on the selected tool diameter (for the modelled tool radius of 25 µm, the resulting change of maximum motion amplitude is 5.9 % at a speed of 90,000 min^{-1}) and the requirements of the application to be manufactured. At node 1 (tool tip location), it can be seen that the maximum motion amplitude changes when comparing the cases without cutting forces and measured cutting forces, showing a process-tool-interaction. While the amplitude change is small in absolute units (< 0.5 µm at all rotational speeds), the relative amplitude change at 30,000 min^{-1} and 90,000 min^{-1} is clearly observable. Additionally, when comparing the case without cutting forces with the cases with scaled cutting forces, it can be seen that the change in terms of maximum motion amplitude becomes significant at all rotational speeds. This indicates that the effect of process-tool-interactions rises with increasing cutting forces. At nodes 2 and 3, it can be seen that the overall trend is similar to that of node 1. The differences are that the maximum motion amplitude reduces in terms of absolute values and in terms of range between no cutting forces and cutting forces. At node 4 (rotor at front bearing location), the difference between the motion amplitudes is less than 0.1 µm between no cutting forces (only rotordynamic effects considered) and 5x scaled cutting forces, independent of the rotational speed.

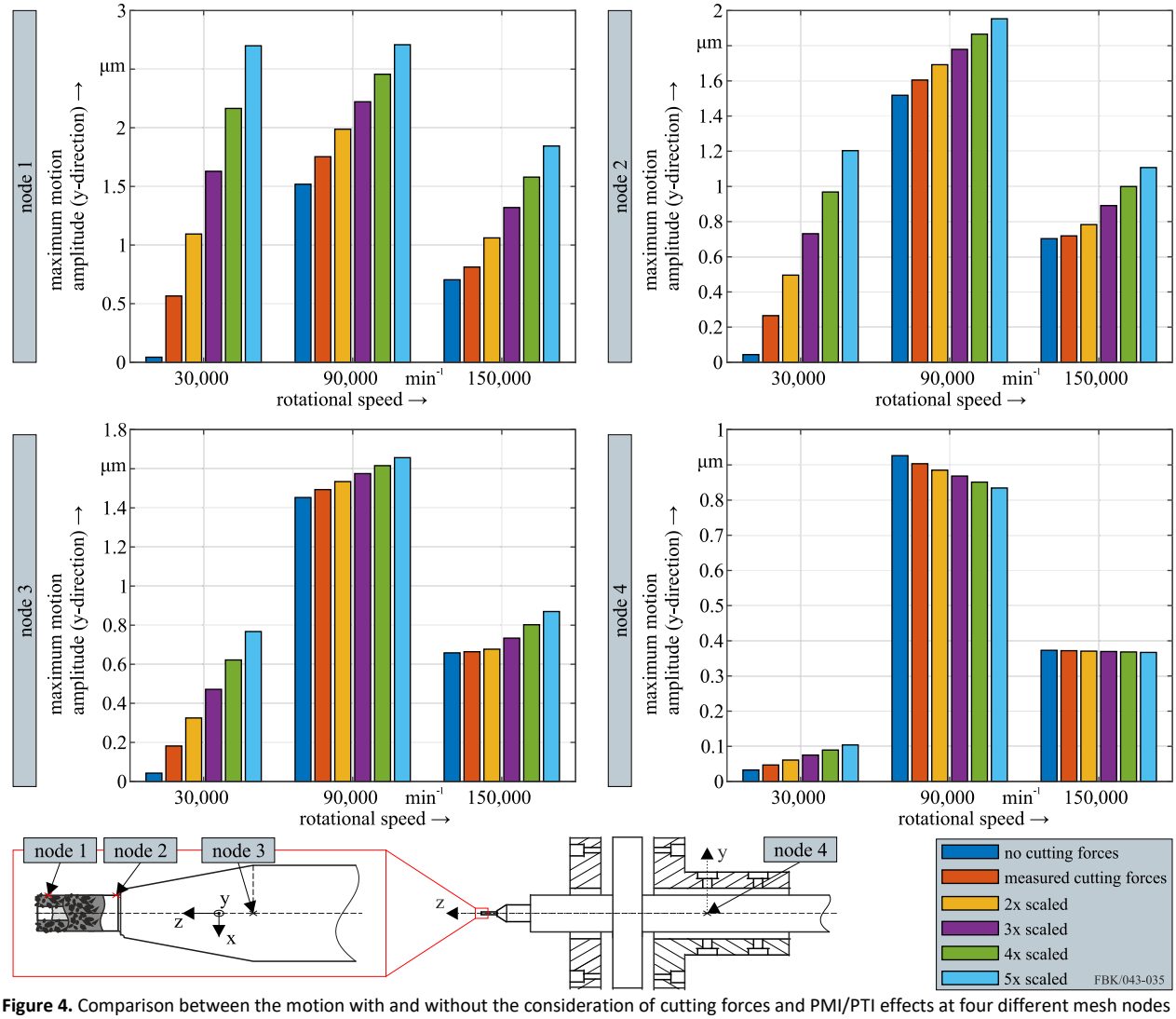

Figure 4. Comparison between the motion with and without the consideration of cutting forces and PMI/PTI effects at four different mesh nodes

Further, at 90,000 min^{-1}, the graph shows that the maximum motion amplitude decreases with increasing cutting forces. This trend is limited to this specific spindle speed and node location and can be attributed to the rotor's bending behaviour. This shows that the rotor's motion itself is not significantly influenced by the cutting forces. This result also corresponds with the comparison between cutting forces and the unbalance force given in table 1.

It still must be determined to what extent the results from figure 4 are based on the variation of the cutting forces due to PMI/PTI effects or on the sole consideration of cutting forces. For this purpose, table 2 lists the maximum motion amplitude at evaluation node 1 with measured (variation of cutting forces due to PMI/PTI effects) and ideal cutting forces (determined as described in section 2.3). The ratio between the results without and with the consideration of PMI/PTI is close to 1, independent of the rotational speed. This suggests that the observed PTI is mainly based on the consideration of the cutting forces but not on the variation of the cutting forces due to additional PMI/PTI effects.

Table 2. Comparison of the tool motion in y-direction at node 1 with measured (variation of forces due to PMI/PTI and tool deformation) and ideal cutting forces (no variation of cutting forces)

rotational speed/min^{-1}	**motion amplitude/µm** no variation of cutting forces due to PTI	**motion amplitude/µm** variation of cutting forces due to PTI	**ratio**
30,000	0.55	0.58	0.95
90,000	1.59	1.75	0.91
150,000	0.82	0.81	1.01

4. Conclusion and outlook

This paper investigated the interaction between tool and workpiece in grinding with micro pencil grinding tools. For this purpose, a coupled simulation model was set up: a dynamic spindle model coupled with a three-dimensional dynamic tool model. Cutting forces were measured and included process-machine-interaction (PMI) and/or process-tool-interaction (PTI) effects as they cannot be omitted during experiments. Idealized cutting forces were computed by curve fitting. For both cases, the forces were implemented as a boundary condition within the coupled simulation model. The motion of the tool and the spindle shaft with and without the consideration of cutting forces and PMI/PTI effects at different mesh nodes was compared.

The following conclusions can be drawn:

- The rotordynamic behaviour of the spindle shaft influences the movement of the tool. Depending on the selected tool diameter and application, this influence can be significant.
- Even with scaled cutting forces, no significant influence of the grinding forces on the spindle dynamics (node 4) can be observed. This shows that in grinding with micro pencil grinding tools, only a process-tool-interaction is observed but no process-machine-interaction.
- Numerical results indicate that the observed PTI is mainly based on the consideration of the cutting forces but not on the variation of the cutting forces due to additional PMI/PTI effects (ongoing cutting force variations due to tool deformation and vice versa).

With the conclusions drawn from this analysis, future works can consider the influence of the spindle dynamics without the need to include the full dynamic machine model. As such, the spindle dynamics can be included in terms of a computed or measured boundary condition in more complex micro grinding simulations, such as kinematic and chip formation simulations used to model the generated workpiece surface. Further, the influence of the number of grits, the grit distribution, and the grit shape on the tool deformation and motion can be analysed without the need to include the full dynamic machine model.

Acknowledgment

This research was funded by the Deutsche Forschungsgemeinschaft (DFG, German Research Foundation) – 252408385 – IRTG 2057.

[1]Naming of specific manufacturers is done solely for the sake of completeness and does not necessarily imply an endorsement of the named companies nor that the products are necessarily the best for the purpose.

References

[1] Denkena B and Hollmann F (Eds.) 2012 Process machine interactions: predicition and manipulation of interactions between manufacturing processes and machine tool structures. Springer Science & Business Media
[2] Brecher C, Esser M, and Witt S 2009 Interaction of manufacturing process and machine tool. *CIRP Annals* **58(2)** 588-607
[3] Afazov S M, Ratchev S M, Segal J, and Popov A A 2012 Chatter modelling in micro-milling by considering process nonlinearities. *International Journal of Machine Tools and Manufacture* **56** 2-38
[4] Reichenbach I G 2017 Beitrag zur Beherrschung der Mikrofräsbearbeitung von Polymethylmethacrylat *Dissertation, Technische Universität Kaiserslautern*
[5] Uhlmann E, Mahr F, Shi Y, and von Wagner, U 2012 Process Machine Interactions in Micro Milling *Process Machine Interactions; Springer, Berlin, Heidelberg* 265-284
[6] Jun M B, Liu X, DeVor R E, and Kapoor S G 2006 Investigation of the dynamics of microend milling—part I: model development *Journal of Manufacturing Science and Engineering* **128(4)** 893-900
[7] Klocke F, Barth S, Wrobel C, Weiß M, Mattfeld P, Brakhage K H, Rom M 2016 Modelling of the grinding wheel structure depending on the volumetric composition *Procedia CIRP* **46** 276-280
[8] Chen X, Li L, Wu Q 2017 Effects of abrasive grit shape on grinding performance. 23rd International Conference on Automation and Computing *IEEE* 1-5
[9] Liu Y, Warkentin A, Bauer R, Gong Y 2013 Investigation of different grain shapes and dressing to predict surface roughness in grinding using kinematic simulations. Precision Engineering **37(3)** 758-764
[10] Heintz M, Arrabiyeh P A, Kirsch B, Aurich J C 2020 Herstellung von Schleifwerkzeugen für die Mikrobearbeitung mithilfe eines chemischen Nickel-Phosphor-Dispersions-Beschichtungsverfahrens. *Jahrbuch Schleifen, Honen, Läppen und Polieren - Verfahren und Maschinen* **69** 16-25
[11] Parker K 1992 Plating and Surface Finishing 29-33
[12] Wiegand H, Heinke G, and Schwitzgibel K K 1968 *Metalloberfläche* **22** 304-311
[13] Arrabiyeh P A, Heintz M, Kieren-Ehses S, Bohley M, Kirsch B, Aurich J C 2020 Submerged micro grinding: a metalworking fluid application study. *The International Journal of Advanced Manufacturing Technology* **107/9-10** 3807-3815
[14] Müller C, Kirsch B, and Aurich J C 2017 Compact Air Bearing Spindles for Desktop Sized Machine Tools *Small Machine Tools for Small Workpieces* 21-34
[15] Lange A, Müller D, Heintz M, Kirsch B, and Aurich J C 2021 Modeling of process-machine-interactions in micro end milling. *Procedia CIRP* **102C** – *Proceedings of the 18th CIRP Conference on Modeling of Machining Operations* 513-518